Angewandte Chemie
Eine Zeitschrift der Gesellschaft Deutscher Chemiker

Supporting Information

Biosynthesis and Mechanism of Action of the Cell Wall Targeting Antibiotic Hypeptin

Daniel A. Wirtz[+], Kevin C. Ludwig[+], Melina Arts, Carina E. Marx, Sebastian Krannich, Paul Barac, Stefan Kehraus, Michaele Josten, Beate Henrichfreise, Anna Müller, Gabriele M. König, Aaron J. Peoples, Anthony Nitti, Amy L. Spoering, Losee L. Ling, Kim Lewis, Max Crüsemann, and Tanja Schneider**

anie_202102224_sm_miscellaneous_information.pdf

SUPPORTING INFORMATION

Table of Contents

SUPPORTING INFORMATION

Experimental Procedures

Purification and isolation of 1

Lysobacter sp. K5869 was grown on 2 % SMS agar containing 10 % R4 broth[1] for 5 days at room temperature. Homogenized colonies of strain K5869 were used to inoculate 250 mL R4 broth supplemented with trace elements. The seed culture was incubated for 5 days at 28°C on a rotary shaker (200 rpm), prior to 5 % (v/v) inoculation of 3 L of fresh medium. Cultures were grown at 28 °C with shaking at 120 rpm for 5 days and screened daily for antibiotic production by using 5 µl of sterile filtered broth supernatant in agar diffusion assays using the cell envelope stress bioreporter *B. subtilis* 168 *amyE*::pAC6 (P_{ypuA}-*lacZ*).[2] At day 3, 60 g of Sepabeads® SP-207 (Sigma-Aldrich) were added to the culture and separated by filtration at day 5. Sepabead-immobilized peptides were extracted with 300 ml of acetone by overnight shaking. The extract was evaporated to dryness and reconstituted in 0.1 % (v/v) aqueous trifluoroacetic acid (TFA). The sample was subjected to reversed-phase high performance liquid chromatography (RP-HPLC) using a preparative MultoKrom® 100-10 C_{18} column (250 × 26 mm, SFD GmbH) eluting with a linear gradient of water and acetonitrile (0-80) + 0.1% (v/v) TFA over 40 min at 10 ml min^{-1} flow rate and UV monitoring at 280 nm. MALDI-TOF profiling indicated the pseudomolecular ion $[M+H]^+$ peaks at 1022.489 *m/z*, indicative of **1** in the 30 - 50 % acetonitrile fractions, which showed bioactivity in agar diffusion assays.
Rechromatography of peak fractions with semipure **1** was carried out by RP-HPLC using three linear gradients of water and acetonitrile with 0 to 30% acetonitrile over a period of 5 min, 30 to 60% acetonitrile over 25 min, and 60 to 80% over 10 min (10 ml min^{-1} flow rate). Rechromatographed fractions were finally lyophilized and resulted in 18.2 mg of pure **1**, leaving a white powder.

SUPPORTING INFORMATION

Cloning, expression and characterization of enzymes

DNA isolation and genome sequencing

Genomic DNA of *Lysobacter sp.* K5869 was prepared from 2 mL freshly grown culture with the GenElute Bacterial Genomic DNA kit (Sigma Aldrich). Sequencing was carried out by Eurofins Genomics (Ebersberg, Germany) with the PAC-BIO SMRT cell technology. After assembly, a single, circular scaffold consisting of 5,968,034 bp was obtained. The location of the chromosomal gene encoding for the replicator protein dnaA of *Lysobacter* was determined and its end position was set to be adjacent to start position 1. The modified scaffold consists out of 5,950,758 bp.

Sequential cloning

Oligonucleotide primers were synthesized by Eurofins Genomics. Primers used for amplification of the different modules of *hynA, hynB*, the genes *hynC*, *hynE*, and *hynMLP* from the genomic DNA of *Lysobacter sp.* K5869 are listed in Table S1. The resulting DNA fragments were cloned into restricted pET28a (*hynABE*) or pCDFDuet-1 (*hynC, hynMLP*) via sequential ligation cloning and transformed into *E. coli* alpha-select silver. The resulting constructs were isolated, analyzed via restriction digest and verified by Sanger DNA sequencing. The final plasmids were then transformed into *E. coli* BL21(DE3) or, when containing a NRPS T domain, into *E. coli* BAP1 for heterologous expression of the His-tagged protein.

Table S1. Primers used for cloning and mutagenesis of enzymes and enzymatic domains of the *hyn* BGC. Restriction sites are bold. Annealing sequences are given in upper case. Mutated nucleotides are underlined.

Name	Sequence (5'→3')
HynA4_Cacc_NdeI_for	tatcatatgGTGAGTGCGCAAGAGCAC
HynA5_Cdon_HindIII_rev	tagaagcttaCAGGCAGCGTCGTTGCCA
HynA5_C2_NdeI_for	tgccatatgGCCTTGTTCGAACCGGCG
HynA5_T_XhoI_rev	tatactcgagttaGCCGTTGGCCGGAACGAC
HynA6_C_NdeI_for	tatcatatgCAGATCGAACGCATCGTC
HynA6_T_HindIII_rev	tagaagcttaCTGACAGTCGACGATGGC
HynB7_A_NcoI_for	tgtccatgggaCGCGAGCAAGTCCTG
HynB7_T_HindIII_rev	tataagcttCTGCCCGACCCGCGCTGCGAA
HynC_BamHI_for	agcggatccATGACCCAGAAGAACTTCAAG
HynC_HindIII_rev	tataagcttTCACAGCAGCAGTTCCCT
HynC_EcoRI_pCDF_for	cacgggaattcgACCCAGAAGAACTTCAA
HynC_HindIII_pCDF_rev	gagaagcttTCACAGCAGCAGTTCCCT
Gib_HynC_E376D_for	tacggcgacCACGCCGATCTCGACAT
Gib_HynC_E376D_rev	cggcgtggTCGCCGTAGAACGGC
HynE_NdeI_for	gcgcatatgATGAGCATGTTCAATCAGCTT
HynE_HindIII_rev	gataagcttCTGGCCCATGCCGACCAG
HynMLP_NdeI_pCDF_for	gcgcatATGAGCAATCCCTTCGACGAC
HynMLP_PacI_pCDF_rev	aatttaattaattAGGCGCCGGGCCGGGC

Site-directed mutagenesis

Gibson assembly[3] was used to introduce specific mutations into the expression plasmids. Primers were designed with an annealing sequence of 18 bp prior to the mutated codon and 10 non-mutated bp to overlap in the assembly (Table S1). Mutated educt fragments were generated from the non-mutated plasmid as template *via* Q5-PCR (NEB). The template DNA was then eradicated by restriction hydrolysis with *dam*$^+$/*dcm*$^+$-methylation sensitive *Dpn*I. 5 µL of the linear PCR products were mixed with 15 µL assembly mixture (5 % PEG-8000, 100 mM Tris-HCl pH 7.5, 10 mM $MgCl_2$, 10 mM DTT, 0.25 mM each of the 4 dNTPs, 1 mM NAD, 0.08 U T5 exonuclease, 0.5 U Phusion polymerase) and incubated at 50 °C for 60 min. After incubation, the whole mixture was used for chemical transformation into *E. coli* alpha-select silver.

SUPPORTING INFORMATION

Protein expression

If the protein of interest included a T domain, the protein expression was conducted in *E. coli* BAP1 to ensure *in vivo* phosphopantetheinylation of the conserved serine residue. All other constructs were expressed in *E. coli* BL21(DE3). Media were supplemented with the appropriate antibiotic, dependent on the respective plasmids in the strain. For the expression of HynC, TB media was additionally supplemented with 25 µM $(NH_4)Fe(III)$-citrate. For the preculture, few mL of LB-broth were inoculated from a cryopreserved culture and incubated overnight (220 rpm, 37 °C). The densely grown preculture was then used in a ratio of 1:100 to inoculate the TB-medium in a baffled Erlenmeyer flask. This expression culture was grown (37 °C, 220 rpm) until OD_{600} = 0.8 and chilled on ice prior to induction with 400 µM isopropyl-β-D-thiogalactopyranoside (IPTG). The cultures were then further incubated at 16 °C and 220 rpm for additional 16 h.
For protein purification, the cells were harvested via centrifugation (10,000 *x g*, 4 °C, 2 min). The pellet was resuspended in 5 mL lysis buffer (50 mM NaH_2PO_4, 300 mM NaCl, pH 8.0) per g pellet and cells were lysed in ice by sonification in 10-seconds intervals. The lysate was centrifuged (12,000 *x g*, 4 °C, 10 min) and the clear supernatant mixed with 1 mL NiNTA agarose per 10 mL supernatant. The suspension was incubated on ice in slight movement. After 1 h, the suspension was filtered with a propylene column (Qiagen, 1 mL or 4 mL). The remaining NiNTA agarose matrix was washed with 4-8 mL 20 mM imidazole buffer and 0-4 mL 35 mM imidazole buffer, depending on the binding affinity of the desired protein. Proteins were eluted with 2.5 mL 250 mM imidazole buffer. The buffer of the elution fraction was exchanged with PD10 columns (Cytiva), following the gravity protocol. If necessary, proteins were concentrated with Amicon® Ultra 4 mL centrifugal filters (Merck) with a molecular weight cut off (MWCO) of at least half the proteins size.

$\gamma^{18}O_4$-ATP exchange assay

Two stock solutions were prepared for the assay. Substrate solution 1: 3 mM of the respective amino acid, 15 mM pyrophosphate in 20 mM Tris pH 7.5; Substrate solution 2: 3 mM $\gamma^{18}O_4$-ATP, 15 mM $MgCl_2$ in 20 mM Tris pH 7.5. 2 µL of each solution were mixed with 2 µL A domain containing protein concentrated to 5 µM in 5 % glycerol, 20 mM Tris pH 7.5 and incubated at 22 °C for 1.5 h. The reaction was stopped by addition of 6 µL 9-aminoacridine in acetone (10 mg/mL). Precipitated proteins were removed via centrifugation. 1 µL of each sample was spotted on the sample carrier and subsequently recrystallized by addition of 0.5 µL acetone. The samples were then analyzed with MALDI-TOF-MS (Bruker AutoFlex III) in negative mode. Absolute substrate conversion in [%] was calculated by dividing the peak area at *m/z* 506 through the combined peak areas at *m/z* 508, 510, 512, and 514, divided by 83.33 for the molar ratio of labelled against unlabeled pyrophosphate in the assay.[4]

In vitro hydroxylation assay with HynE

The phosphopantetheinylated NRPS modules $HynA_4C_{acc}ATC_{don}$, $HynA_5CAT$, $HynA_6CAT$ or $HynB_7AT$ were purified from *E. coli* BAP1 as described above and buffered in 50 mM Tris pH 7.5, 150 mM NaCl, 10 mM $MgCl_2$ using PD-10 columns. The assay was performed in a 500 µL one-pot-reaction: 50 µM HynE and 50 µM NRPS module were supplemented with 1 mM ATP, 1 mM of the respective amino acid, 5 mM DTT and 0.5 mM of each $(NH_4)_2Fe(SO_4)$, α-ketoglutarate and ascorbate. The reaction was incubated with slight movement for 3 h at 20 °C. Afterwards, the reaction was quenched by adding 50 µL 100 % (w/v) TCA and incubated for 30 min on ice. The precipitated proteins were washed twice with buffer after careful centrifugation (9000 *x g*, 5 min). Alkaline thioester cleavage was conducted with 200 µL KOH (0.1 M) at 70 °C for 20 min. The solution was lyophilized and the pellet dissolved in a minimal volume of ddH_2O for LC-MS analysis. As a negative control, HynE was heat-inactivated at 80 °C for 10 min prior to addition of the NRPS module and the substrates.
Analysis of the amino acids was performed on a Waters e2695 separation module, coupled to an Acquity QDa and 2998 PDA detector with a NUCLEODUR® HILIC 250x4.6 column as stationary phase. Elution was conducted with an isocratic gradient of Acetonitrile:5 mM aminoacetate pH 7.4 70:30 at a flow of 0.7 mL/min over 20 min. Amino acids were detected in negative mode.

In vitro hydroxylation assay with HynC

Heterologously expressed HynC was only stable, when co-expressed and purified with the respective NRPS module. The enzymes were purified from *E. coli* BAP1 and buffered in 50 mM Tris pH 7.5, 150 mM NaCl, 10 mM $MgCl_2$ using PD-10 columns. Afterwards, the protein mass was roughly determined by measuring the absorption at λ=280 nm. 500 µL of the solution with 5.0 mg/mL protein were supplemented with 1 mM ATP, 1 mM of the respective amino acid, 10 µM methylviologen and 1 mM NADH and incubated with slight movement at 20 °C overnight. Alkaline thioester cleavage, further processing, and analysis of the sample were conducted as described above.

SUPPORTING INFORMATION

Bioinformatic analysis of $HynA_5C_2$

For phylogenetic analysis of the condensation domain superfamily, the datasets from Rausch et al.[5] and Reitz et al.[6] together with homologues of $HynA_5C_2$ were imported to MEGA-X.[7] Multiple sequence alignment was performed using the MUSCLE-algorithm. The maximum-likelihood tree was constructed using the Dayoff matrix based model. The tree with the highest log likelihood (-36592.07) is shown in Figure S3. The Initial tree for the heuristic search was obtained automatically by applying Neighbor-Join and BioNJ algorithms to a matrix of pairwise distances estimated using a JTT model, and then selecting the topology with superior log likelihood value. A discrete Gamma distribution was used to model evolutionary rate differences among sites (5 categories (+G, parameter = 2.1883)). The tree is drawn to scale, with branch lengths measured in the number of substitutions per site. All positions with less than 95 % site coverage were eliminated. Branch support was assessed by bootstrapping with 100 replicons.

SUPPORTING INFORMATION

Bioactivity of 1

Antibiotic susceptibility testing

MIC was determined by broth microdilution according to CLSI guidelines, in polypropylene microtiter plates (Nunc brand) using cation-adjusted Mueller-Hinton broth (MHB, Oxoid).

Killing kinetics

S. aureus SA113 was grown in MHB at 37 °C to exponential phase (OD_{600} = 0.5) or stationary phase (OD_{600} = 1). Bacteria were challenged with **1** at 1× and 2× MIC. Vancomycin and teixobactin (both 10× MIC) served as positive controls. At defined time points aliquots were taken, centrifuged at 10,000 × *g* for 1 min, and resuspended in sterile phosphate buffered saline (PBS). Tenfold serially diluted suspensions were spotted as triplicates on Mueller Hinton agar (MHA) plates. CFU ml^{-1} were determined after overnight incubation at 37 °C.
For visual analysis of lysis in microtiter plates, stationary phase cells (OD_{600} = 1) cells of *S. aureus* SA113 and the AtlA-deficient mutant *S. aureus* SA113 Δ*altA* (supplemented with 150 µg ml^{-1} spectinomycin) were treated with **1**, teixobactin, and vancomycin at concentrations of 2×, 5× and 10× the MIC and were photographed after 24 h. Experiments were performed with three biological replicates.

β-galactosidase reporter assays

B. subtilis β-galactosidase reporter assays were performed as previously described.[2] In short, reporter strains were grown in MHB containing 5 µg/ml chloramphenicol at 30 °C to an OD_{600} of 0.5. Subsequently, cells were poured at 1 × 10^7 CFU ml^{-1} in MHA plates supplemented with 5 µg/ml chloramphenicol, 75 µg/ml (cell wall reporter), 125 µg/ml (DNA reporter), and 250 µg/ml (RNA and protein reporters) X-gal, respectively. After solidification of the plates, 5 µg of **1** and control antibiotics inducing the promotors were spotted (6 µg vancomycin for cell wall, 0.3 µg ciprofloxacin for DNA, 6 µg rifampicin for RNA, 3 µg clindamycin for protein). Results were documented after incubation overnight at 30 °C.

Luciferase reporter assays

B. subtilis luciferase reporter assays were conducted as previously described.[8] Briefly, *B. subtilis* P_{lial}-*lux* was grown in MHB containing 5 µg/ml chloramphenicol at 30 °C to an OD600 of 0.5. Cells were added to 96-well white wall chimney plates containing serially diluted antibiotics. Luminescence measurements were performed at 30 °C in a microplate reader Spark 10M (Tecan). At least three independent biological replicate experiments were conducted.

[^{3}H]-glucosamine incorporation studies

The effect of **1** on cell wall synthesis was studied by monitoring the incorporation of [^{3}H]*N*-acetyl-glucosamine (GlcNAc); 0.02 MBq ml^{-1} into the acid-precipitable cell fractions as previously described.[9] MHB-grown cultures of *S. simulans* 22 were treated with **1** at 1× MIC, and with vancomycin at 10× MIC.

Bacterial cell wall integrity assay

Bacterial cell wall integrity assays were adapted from previous work.[10] *B. subtilis* 168 cultures were grown in MHB at 30 °C to an OD_{600} of 0.3. Subsequently, cells were treated with 0.625 µg/ml **1**, 0.2 µg/ml teixobactin, 2 µg/ml vancomycin, 4 µg/ml plectasin, 256 µg/ml ampicillin, and further incubated at 30 °C for 90 min. Lysozyme-treated (128 µg/ml) cells were incubated for 10 min. Cells were immediately fixed with in a 1 ml 1:3 (v:v) mixture of acetic acid and methanol, and immobilized on thin 1 % w/v agarose slides. Imaging was performed by phase contrast microscopy on a Zeiss Axio Observer Z1 microscope (Zeiss, Jena, Germany) equipped with HXP 120 V light source and an Axio Cam MR3 camera. Images were acquired with ZEN 2 software (Zeiss) and analyzed and postprocessed using ImageJ v1.45s software (National Institutes of Health).[11]

SUPPORTING INFORMATION

MinD delocalization studies

B. subtilis 1981 *erm spc minD*::*ermC amyE*::P_{xyl}-*gfp-minD*, a strain with a *gfp-minD* fusion under control of the P_{xyl} promotor,[12] was grown in MHB supplemented with 0.1 % w/v xylose and 50 µg/ml spectinomycin at 30 °C to an OD_{600} of 0.6. Imaging was carried out within 2, 30, and 120 min after addition of **1** at 2× and 10× MIC. The proton ionophore carbonyl cyanide *m*-chlorophenylhydrazone (CCCP, 100 µM) was used as positive control and imaging was carried out within 2 min. Samples were immobilized on microscope slides covered with 1 % w/v agarose. Fluorescence microscopy and analysis was performed using the same microscope and software as described for phase contrast microscopy.

Determination of the membrane potential

The membrane potential was determined as previously described,[13] using the lipophilic cation tetraphenylphosphonium (TPP^+), which diffuses across the bacterial membrane in response to a trans-negative membrane potential (ΔΨ). 1 µCi/ml [^{3}H]TPP+ (26 Ci/mmol) was added to a culture of *S. simulans* 22 with an OD_{600} of 0.7 in half-concentrated MHB at 37 °C. The culture was treated with **1** at 1×, 2× and 5× MIC or with 500 µM of CCCP as positive control. Samples of 100 µl were filtered through 0.2 µm cellulose acetate filters and washed twice with 5 ml of 200 mM potassium phosphate buffer. Filters were dried and counted. For calculation of ΔΨ, cell-associated versus free TPP^+ concentrations were applied to the Nernst equation $\Delta\Psi = (-2.3 \times R \times T/F) \times \log(TPP^+_{in}/TPP^+_{out})$ where T is absolute temperature, R is the universal gas constant, and F is the Faraday constant. Mean ΔΨ values were calculated from three independent determinations.

Potassium release from whole cells

The potassium release assays were adapted as previously described.[10] Briefly, tryptic soy broth (TSB)-grown *S. simulans* 22 cells were harvested at an OD_{600} of 1.0 to 1.5, washed with cold choline buffer (300 mM choline chloride, 30 mM MES, 20 mM Tris, pH 6.5), and resuspended to an OD_{600} of 30. The concentrated cell suspension was kept on ice and used within 30 min. For each measurement, the potassium electrode (Mettler Toledo) was calibrated with potassium chloride. Cells were diluted in choline buffer at RT to an OD_{600} of 3, and the peptide-induced potassium release was monitored in 15 sec intervals for 5 min at RT. **1** was added in a concentration corresponding to 1× MIC. Potassium concentrations were calculated from the measured voltage according to Orlov *et al.*[14] and plotted relative to the total amount of potassium released after the addition of 1 µM of the pore-forming lantibiotic nisin (set 100 % efflux). Results show mean values of three independent experiments.

Quantification of intracellular UDP-N-acetylmuramic acid-pentapeptide (UDP-MurNAc-pp)

To analyze the cytoplasmic nucleotide pool we adapted the protocol of Kohlrausch and Höltje.[15] *S. aureus* SG511 was grown in 15 ml MHB at 37°C to an OD_{600} of 0.6 and incubated with 130 µg/ml chloramphenicol for 15 min. **1** was added at 1×, 2.5×, and 5× MIC and incubated for another 30 min. Lipid II-complexing vancomycin (5× MIC) was used as positive control. Extraction of nucleotide-linked PGN precursors and their analysis was performed by HPLC as described previously.[16] Corresponding fractions were confirmed by mass spectrometry.

Synthesis and purification of lipid intermediates

Large scale synthesis and purification of the PGN precursors lipid I, lipid II, and the wall teichoic acid precursor lipid III_{WTA} were performed as previously described.[17] UDP-*N*-acetyl-muramic acid pentapeptide (UDP-MurNAc-pp) was purified according to the protocol elaborated by Kohlrausch and Höltje.[15] Geranylgeranyl phosphate ($C_{20}P$), undecaprenyl phosphate ($C_{55}P$), geranylgeranyl diphosphate ($C_{20}PP$), and undecaprenyl diphosphate ($C_{55}PP$) were purchased from Larodan Fine Chemicals AB (Malmö, Sweden), 1,2-dioleoyl-sn-glycero-3-phosphoglycerol (DOPG) was purchased from Avanti Polar Lipids (Alabaster, AL, USA) The concentration of purified PGN and wall teichoic acid precursors was quantified on the basis of their phosphate content as described.[18]

SUPPORTING INFORMATION

In vitro lipid II synthesis with isolated membranes

In vitro lipid II synthesis was performed using membranes of *M. luteus* as previously described.[19] Briefly, synthesis was assayed by incubating membrane preparations (200 µg protein) with 5 nmol $C_{55}P$, 50 nmol UDP-MurNAc-pp, 50 nmol UDP-*N*-acetylglucosamine (UDP-GlcNAc), and 0.5 nmol [^{14}C]UDP-GlcNAc in 60 mM Tris-HCl, 5 mM $MgCl_2$, and 0.5 % Triton X-100, at pH 7.5 in a total volume of 50 µl at 30 °C for 1 h. $C_{55}P$-containing products were extracted with an equal volume of *n*-butanol/pyridine acetate, pH 4.2 (2:1, v/v) and analyzed by TLC using chloroform/methanol/water/ammonia (88:48:10:1, v/v/v/v) as the solvent[20] and phosphomolybdic acid staining.[21] The quantitative analysis of lipids extracted to the butanol phase was carried out by phosphorimaging in a StormTM imaging system (GE Healthcare) or PMA staining and analysis performed using Image Quant TL. **1** was added in molar ratios of 0.5 to 2 with regard to $C_{55}P$.

In vitro PGN synthesis reactions using purified proteins and substrates

The synthesis of lipid II-Gly_1 catalyzed by FemX was performed in a 100 µl reaction containing 1 nmol lipid II, 2 mM ATP, 25 µg tRNA, 0.1 mM glycine, 50 nmol [^{14}C]glycine in 100 mM Tris-HCl, 20 mM $MgCl_2$, 0.8 % Triton X-100, at pH 7.5 with 2.7 µg FemX and 10 µg GlyS. The reaction mixtures were incubated for 30 min at 30°C.
The lipid IV_{WTA} synthesis reaction was determined by incubating 2 nmol of lipid III_{WTA} in 200 mM Tris-HCl, 0.2 % Triton X-100, 100 mM NaCl, and 1 mM UDP-GlcNAc, at pH 7.5 in 50 µL. The reaction was initiated by the addition of 3 µg of TarA-His_6 and 1 µg MnaA-His_6 and incubated for 4 h at 30 °C.
Dephosphorylation of $C_{55}PP$ was determined using purified *S. aureus* YbjG-His_6 enzyme. 20 nmol of $C_{55}PP$ were incubated with 3 µg of YbjG-His_6 in 20 mM Tris-HCl, 150 mM NaCl, and 0.8 % Triton X-100 at pH 7.5 in 50 µL for 30 min at 37 °C.
In all *in vitro* assays, **1** was added in molar ratios from 0.5 to 2 with respect to the respective substrate. $C_{55}P$-containing products were extracted, analyzed by TLC and quantified as described above. Experiments were performed at least three times.

*Complex formation of **1***

Binding of **1** to $C_{55}P$, $C_{55}PP$, lipid I, lipid II, and lipid III_{WTA} was analyzed by incubating 2 nmol (5 nmol for $C_{20}PP$ and $C_{55}PP$) of each cell wall precursor with 1 to 4 nmol (2.5 to 10 nmol) of **1** in 50 mM Tris-HCl, at pH 7.5 for 30 min at RT. Complex formation was analyzed by extracting unbound precursors from the reaction mixture followed by TLC analysis as described above. Experiments were performed with biological replicates.

Antagonization assays

Antagonization of the antibiotic activity of **1** and teixobactin by potential target molecules was performed by an MIC-based setup in microtiter plates. Both antibiotics (4× MIC) were mixed with HPLC-purified antagonists ($C_{20}P$, $C_{55}P$, $C_{20}PP$, $C_{55}PP$, lipid I, lipid II, lipid III_{WTA}, and DOPG) in 0.00156 to 16-fold molar excess with respect to the antibiotic. *S. aureus* SG511 (5×10^5 CFU ml^{-1}) was added and samples were examined for visible bacterial growth after incubation overnight. Experiments were performed with biological replicates.

Mammalian cytotoxicity

Cytotoxicity of **1** on human epithelial type 2 (HEp-2) cells (ATCC® CCL-23™) was measured by using the non-fluorescent resazurin-based alamarBlue™ cell viability reagent (Invitrogen) which is converted into fluorescent resorufin by living cells. HEp-2 cells were seeded at a density of 5×10^4 cells per well in 96-well flat base TC plates (Sarstedt), and incubated in Dulbecco's modified Eagle's medium (DMEM, Gibco) supplemented with 1× MEM non-essential amino acids (Gibco) and 1× MEM vitamin solution (Gibco) in an atmosphere of 5 % CO_2 at 37 °C. After 48 h, the culture was treated with **1** at serially diluted concentrations ranging from 1 to 128 µg/ml. After another incubation for 30 h, medium was removed and the cell monolayer was washed twice with Hank's balanced salt solution (HBSS, Gibco). To indicate cell viability, alamarBlue™ reagent was added to a final concentration of 10 % (v/v) and cells were incubated for 1 h at 37 °C and 5 % CO_2. Fluorescence measurements (570 nm excitation and 585 nm emission) were performed in black F-bottom microplates (FLUOTRAC, Greiner) with a microplate reader Spark 10M (Tecan). Relative cell viability was calculated as the percentage of untreated cells (set 100 %).

SUPPORTING INFORMATION

Red blood cell lysis assay

1 and teixobactin were serially diluted in phosphate buffered saline (PBS) in 96-well U-shaped plates (Greiner) at concentrations ranging from 1 to 128 µg/ml. Human red blood cells (RBCs) were washed three times with PBS immediately prior to addition of RBCs to the wells at a final concentration of 2.5 % RBC per well. After 6, 17, or 30 h of incubation in an atmosphere of 5 % CO_2 at 37°C, RBCs were pelleted by centrifugation (1500 × *g* for 10 min). Supernatants were diluted 5-fold in PBS in a new 96-well plate, and absorbance of the heme was measured at 405 nm in a microplate reader Spark 10M (Tecan). Relative hemolysis was calculated as the percentage of RBCs treated with 1 % (v/v) Triton X-100 (set 100 %).

Serial passaging

S. aureus SG511 was serially passaged in the presence of sub-MIC concentrations of **1** over a period of 30 days. Cells were incubated at 37 °C with agitation and passaged at 24 h intervals in the presence of **1** at subinhibitory concentration. The well containing bacterial suspension at the **1** concentration corresponding to 0.5× MIC was used as the inoculum for the second passage. For each passage, MICs were determined as described for *Antibiotic susceptibility testing*.

Results and Discussion

Structural analysis of 1

Hypeptin (1): white, solid; $[\alpha]^{25}_{D}$ −14.5 (*c* 0.2, MeOH); UV (MeOH) λ_{max} (ε) 227 (8170), 289 (1800), 303 (1590) nm; IR (ATR) ν_{max} 3279, 1660, 1651, 1519, 1454, 1199, 1135, 839, 799, 721 cm^{-1}; ^{1}H NMR and ^{13}C NMR data, see Table S2; MALDIMS *m*/*z* 1022.489 $[M+H]^{+}$ (calcd for $C_{44}H_{72}N_{13}O_{15}$, 1022.527).

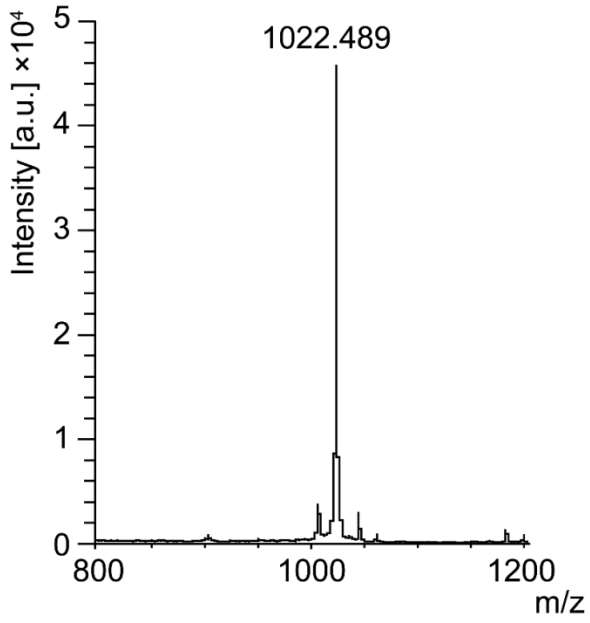

Figure S1. MALDI MS spectrum of **1**.

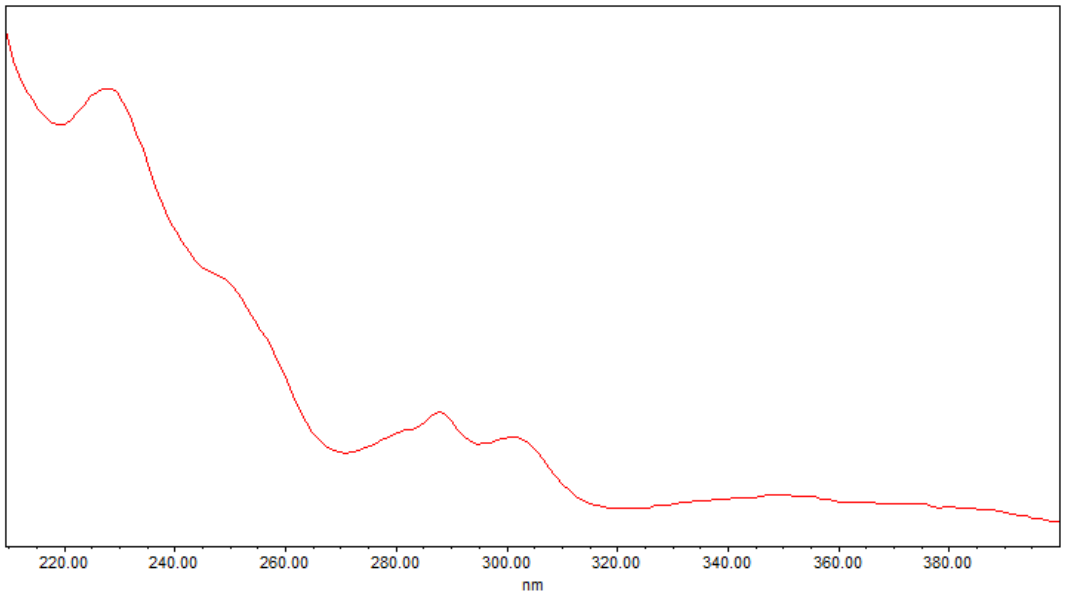

Figure S2. UV spectrum of **1** in MeOH.

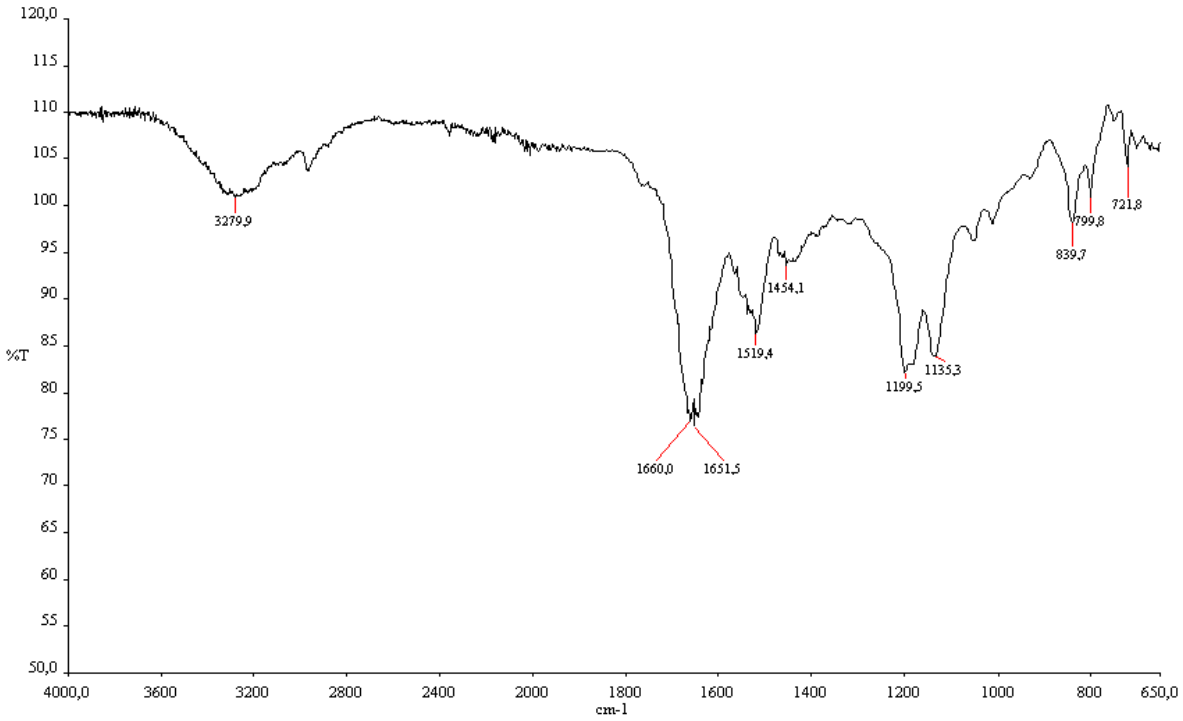

Figure S3. FT-IR spectrum of **1**.

Table S2. ^{1}H and ^{13}C NMR spectroscopic data of **1** (see Supplementary Figures S4-S11) in DMSO-d_6 at 40 °C (^{1}H: 600 MHz; ^{13}C: 150 MHz).

	C/H no.	δ_H (*J* in Hz)[a]	δ_C[a]	HMBC	ROESY
Ala	1		169.4, C		
	2	3.99, m	48.6, CH		3, NH_2-2, NH-5
	3	1.41, d (7.1)	16.9, CH_3		2, NH_2-2, NH-5
	NH_2-2	8.10, m		1	2, 3
Leu	4		171.1, C		
	5	4.40, m	51.3, CH	1, 4	6a/b, 8, NH-5, NH-11
	6	a: 1.55, m	40.3, CH_2		
		b: 1.69, m			
	7	1.63, m	24.4, CH		
	8	0.89, d (6.4)	20.8, CH_3		
	9	0.92, d (6.4)	23.0, CH_3		
	NH-5	8.67, d (8.0)		1	2, 3, 5, NH-11, NH-17
Arg	10	-	171.2, C		
	11	4.44, q (7.6)	55.2, CH	4, 10	12a/b, 13, 14, NH-11
	12	a: 1.70, m	28.9, CH_2		
		b: 1.93, m			
	13	1.55, m	24.5, CH_2		
	14	3.11, m	40.2, CH_2		13, NH-15
	15		156.7, C		
	NH-11	8.11, m		4	5, 12a, 13, NH-5
	NH-15	7.61, brs			
Has	16	-	169.0, C		
	17	4.82, dd (3.5, 10.0)	56.3, CH	10, 16, 19	18, NH-17
	18	4.36, m	72.3, CH	16, 19	17
	19	-	173.5, C		
	OH-18	6.25, brs			
	NH-17	8.16, d (10.0)			11, 17
	NH_2-19	a: 7.37, brs			NH-19b
		b: 7.62, brs			NH-19a
Has	20	-	167.6, C		
	21	5,13, dd (2.5, 10.0)	53.6, CH	16, 20	22, NH-21, NH_2-23, NH-37
	22	5.40, d (2.5)	72.7, CH	20, 23, 24	21, NH-21, NH_2-23
	23	-	168.6, C		
	NH-21	8.15, d (10.0)		16	21, NH-37
	NH_2-23	a: 7.18, brs			NH-23b
		b: 7.69, brs			NH-23a
Ile	24	-	168.7, C		
	25	4.14, t (9.6)	56.6, CH	24, 30	26, 27a/b, 28, 29, NH-25
	26	1.95, m	36.0, CH		
	27	a: 1.18, m	24.4, CH_2		
		b: 1.55, m			
	28	0.80, t (7.5)	10.0, CH_3		25, 26
	29	0.89, d (6.7)	14.9, CH_3		25, 26
	NH-25	8.02, d (9.6)		30	25, 26, 32, NH-31
Hle	30		169.6, C		
	31	4.34, dd (6.4, 10.4)	57.7, CH	30, 36	32,33,34,35, NH-25, NH-31
	32	3.58, m	75.1, CH		31, 33, 34, 35
	33	1.60, m	30.4, CH		
	34	0.71, d (6.7)	19.3, CH_3		31, 32, 33, 35
	35	0.92, d (6.4)	17.1, CH_3		31, 32, 34
	OH-32	5.77, brs			
	NH-31	8.33, brs		36	31, 32, 33, 38, NH-25
Hty	36	-	168.8, C		
	37	4.23, t (7.2)	63.3, CH	20, 36	38, 40, NH-37
	38	4.80, d (7.2)	71.6, CH	36	33, 35, 37, 40, 44
	39		130.8, C		
	40	7.12, d (8.2)	127.8, CH		33, 34, 35, 37, 38, 41
	41	6.63, d (8.2)	114.4, CH		34, 40
	42		156.5, C		
	43	6.63, d (8.2)	114.4, CH		44
	44	7.12, d (8.2)	127.8, CH		43
	OH-38	6.25, brs			
	OH-42	9.20, brs			
	NH-37	8.32, d (7.2)		20	21, 37, 38, 44, NH-21

[a] assignments are based on extensive 1D and 2D NMR measurements (HMBC, HSQC, COSY)

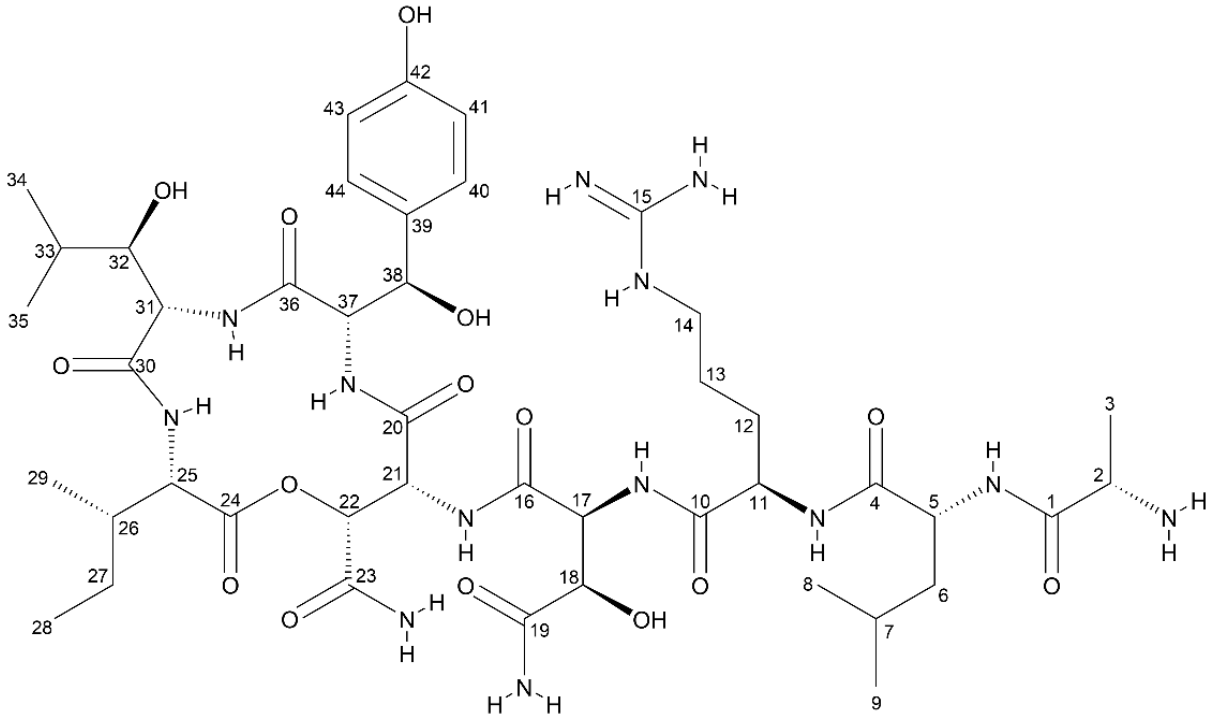

Figure S4. Chemical structure of **1**. Carbon atoms are numbered.

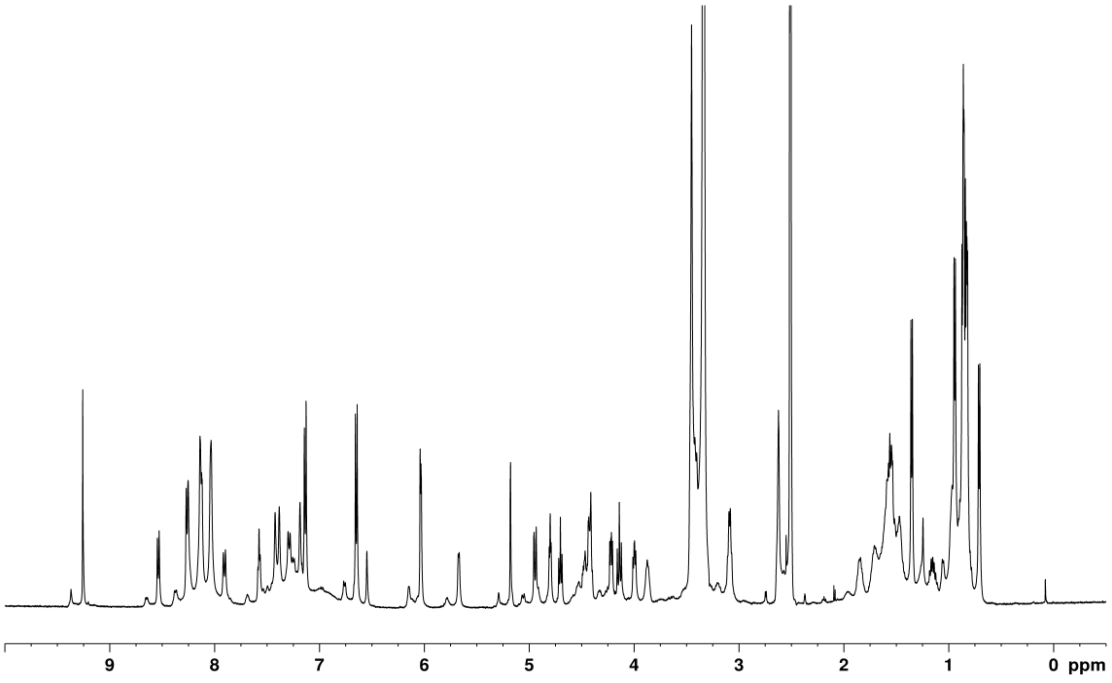

Figure S5. ^{1}H NMR spectrum of **1** in DMSO-d_6 (700 MHz).

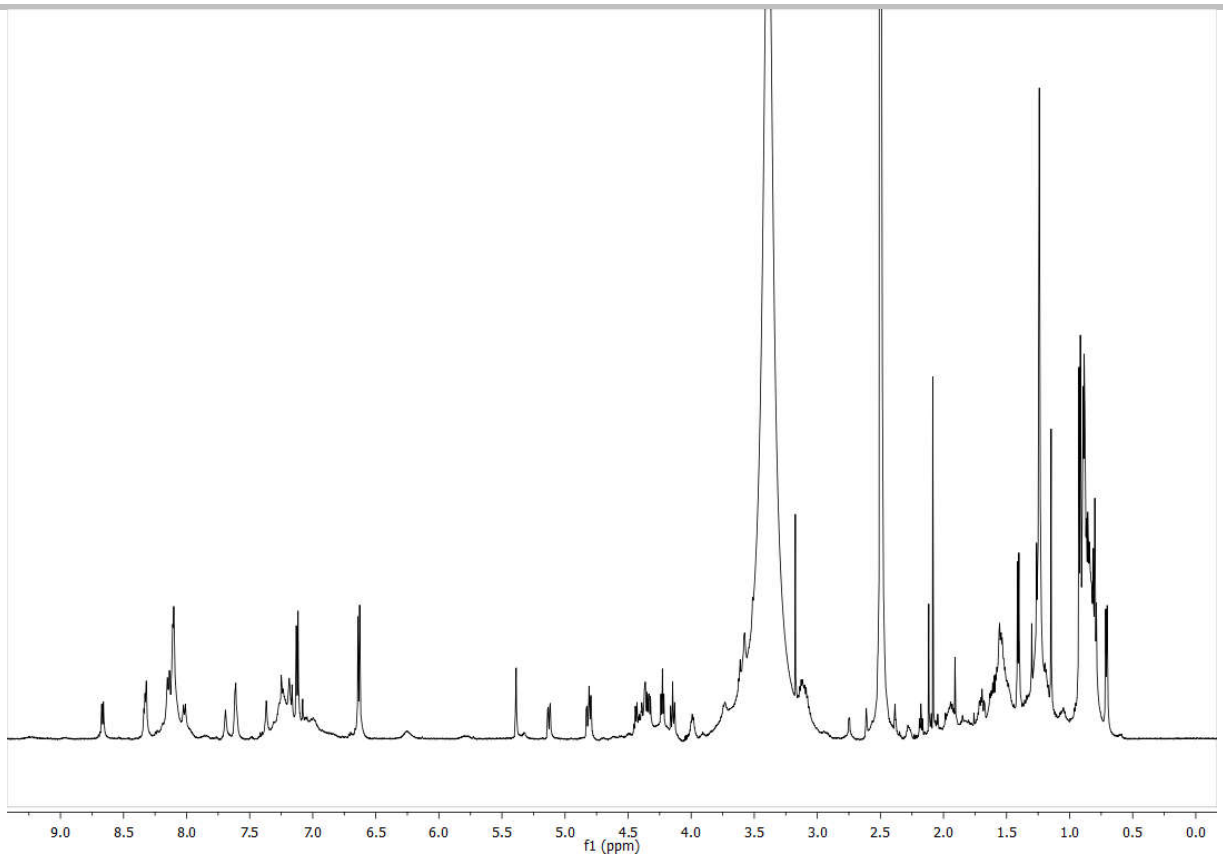

Figure S6. ^{1}H NMR spectrum of **1** in DMSO-d_6 (600 MHz, 40 °C).

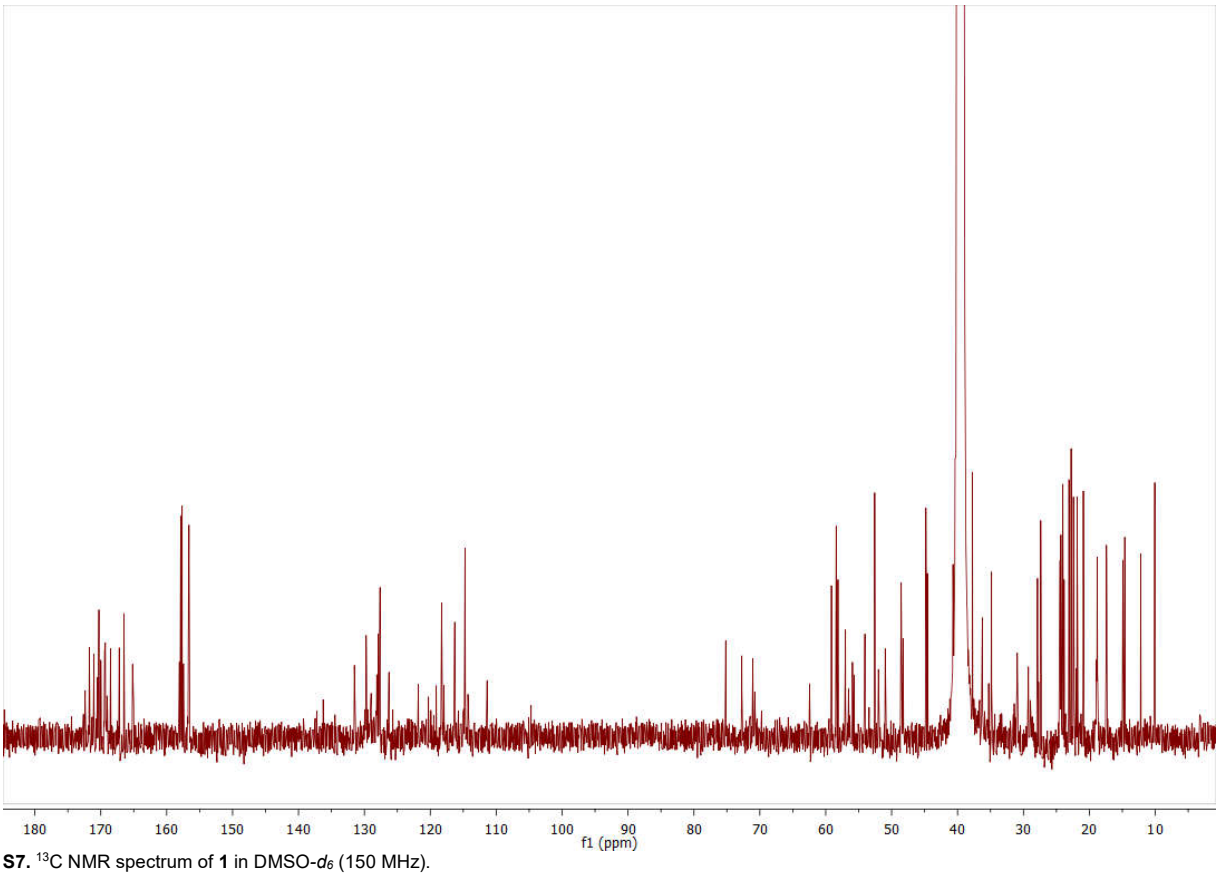

Figure S7. ^{13}C NMR spectrum of **1** in DMSO-d_6 (150 MHz).

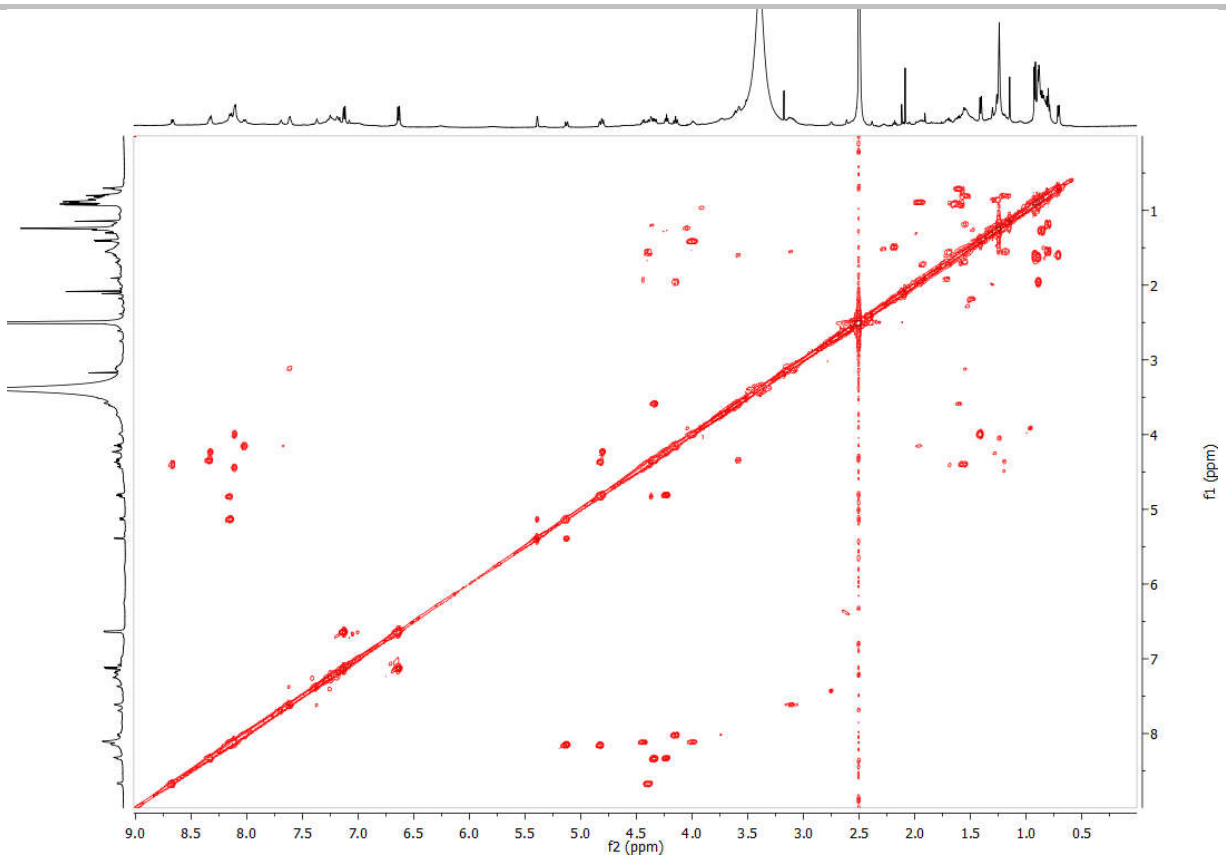

Figure S8. ^{1}H-^{1}H COSY spectrum of **1** in DMSO-d_6 (600 MHz).

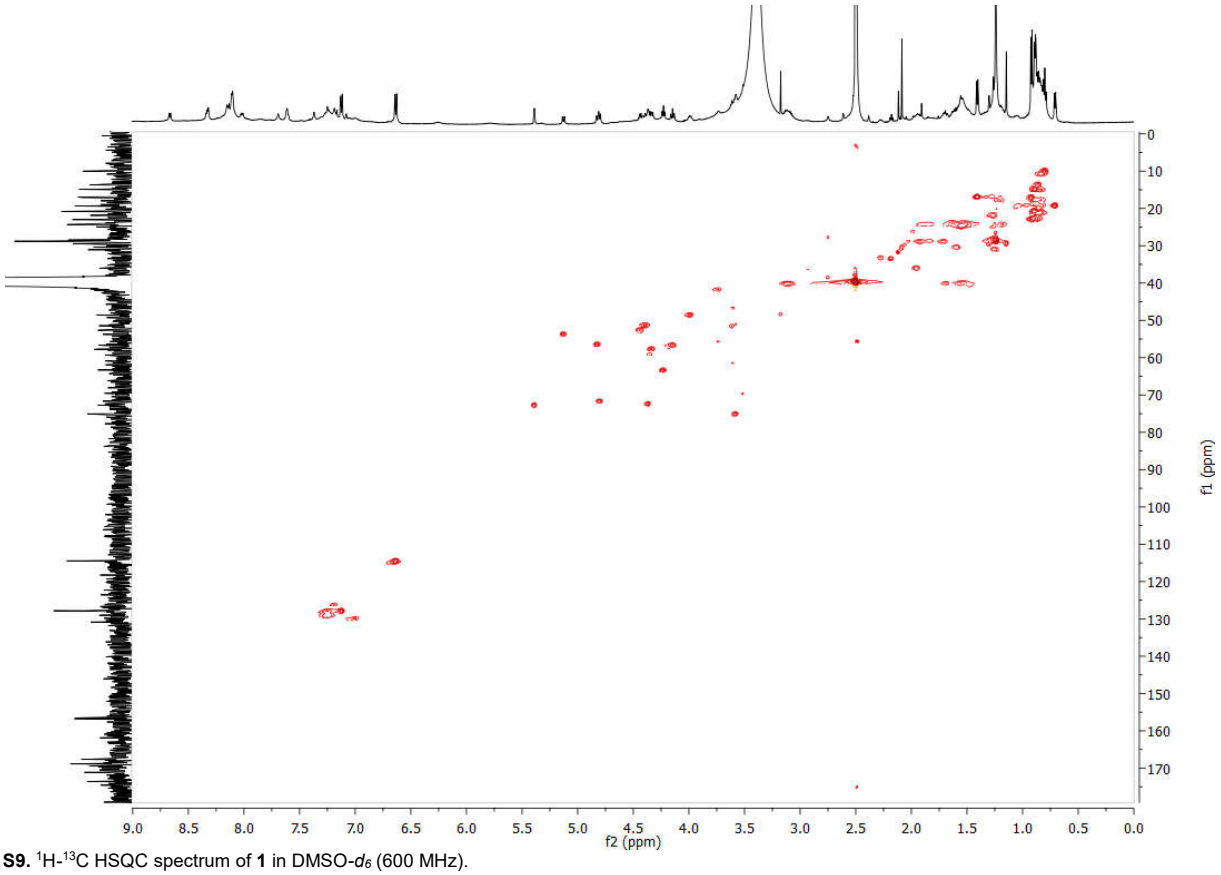

Figure S9. ^{1}H-^{13}C HSQC spectrum of **1** in DMSO-d_6 (600 MHz).

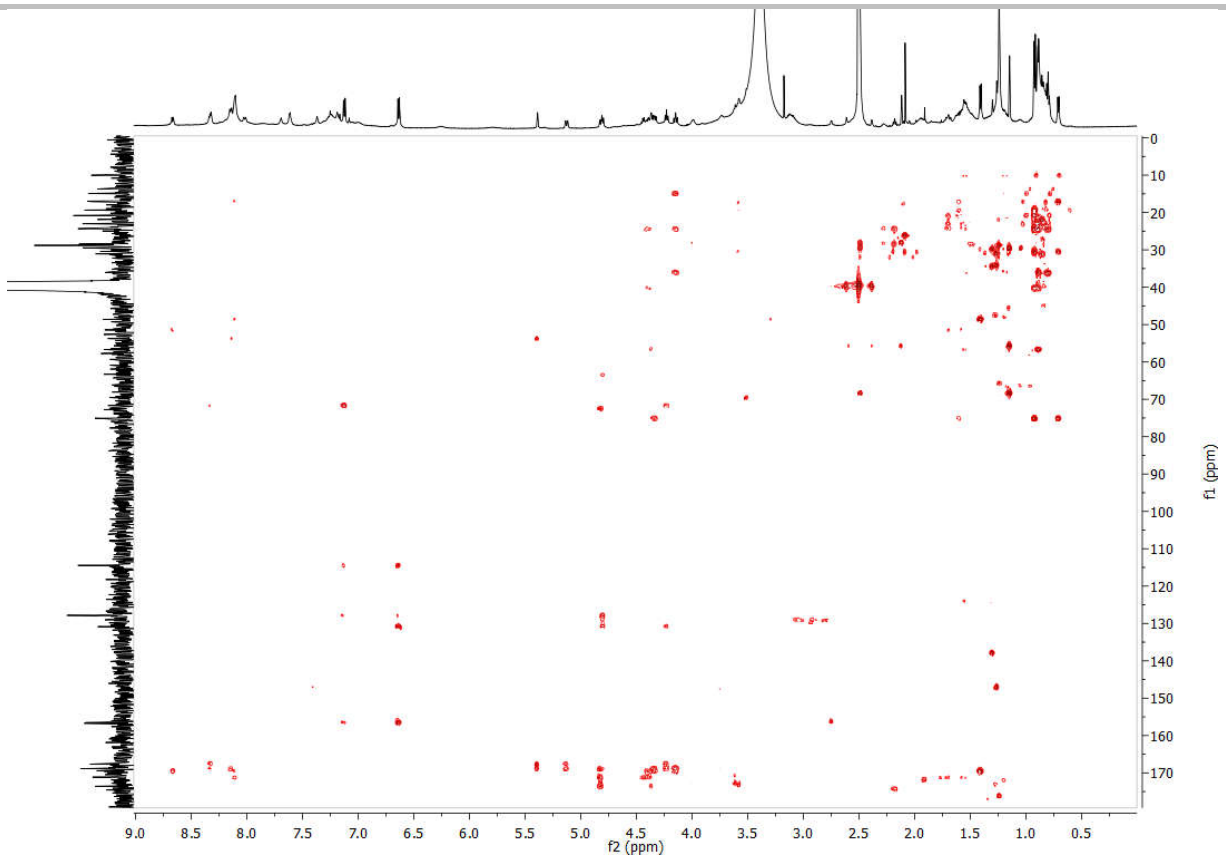

Figure S10. ^{1}H-^{13}C HMBC spectrum of **1** in DMSO-d_6 (600 MHz).

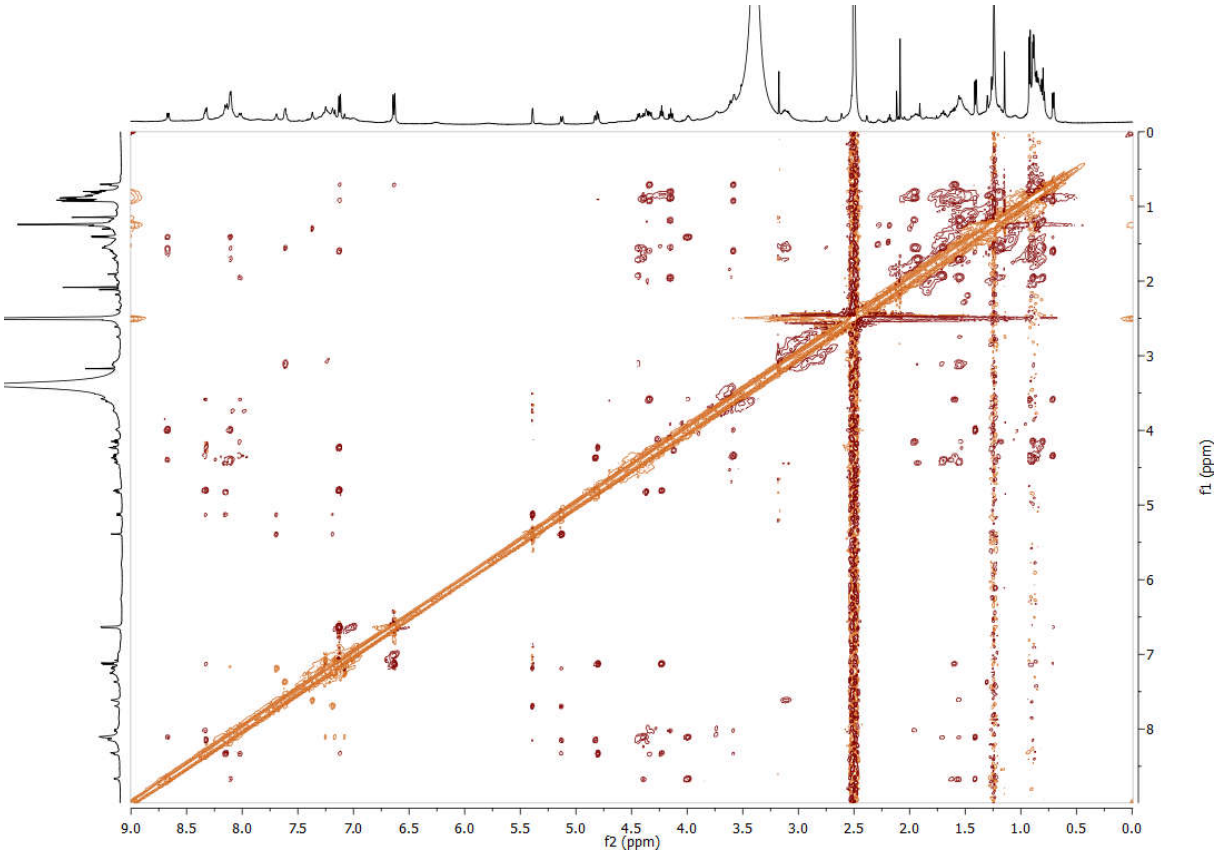

Figure S11. ^{1}H-^{1}H ROESY spectrum of **1** in DMSO-d_6 (600 MHz).

SUPPORTING INFORMATION

Biosynthesis of 1

Table S3. Top BLAST hits of the single genes of the *hyn* BGC (NCBI Accession Number BankIt2428365 MW759775).

Name	Size (aa)	Annotated function	Closest homologue (identity [%])	Accession No. of the homologue
HynA	6491	NRPS	Amino acid adenylation domain-containing protein [*Lysobacter psychrotolerans. ZS60*] (80)	WP_123088455.1
HynB	2447	NRPS	Non-ribosomal peptide synthetase [*Lysobacter psychrotolerans ZS60*] (82)	WP_123088454.1
HynC	531	Non-heme diiron monooxygenase	MBL fold metallo hydrolase [*Lysobacter psychrotolerans ZS60*] (92)	WP_123088453.1
HynD	608	ABC-transporter related protein	ATP-binding cassette domain-containing protein [*Lysobacter psychrotolerans ZS60*] (81)	WP_148041022.1
HynE	302	α-ketoglutarate dependent oxygenase	TauD/TfdA family dioxygenase [*Lysobacter psychrotolerans ZS60*] (83)	WP_123088451.1
HynF	401	RND family efflux transporter MFP subunit	Efflux RND transporter periplasmic adaptor subunit [*Lysobacter psychrotolerans ZS60*] (72)	WP_123088450.1
HynG	1028	AcrB/AcrD/AcrF family protein	Efflux RND permease subunit [*Lysobacter psychrotolerans ZS60*] (80)	WP_123088449.1

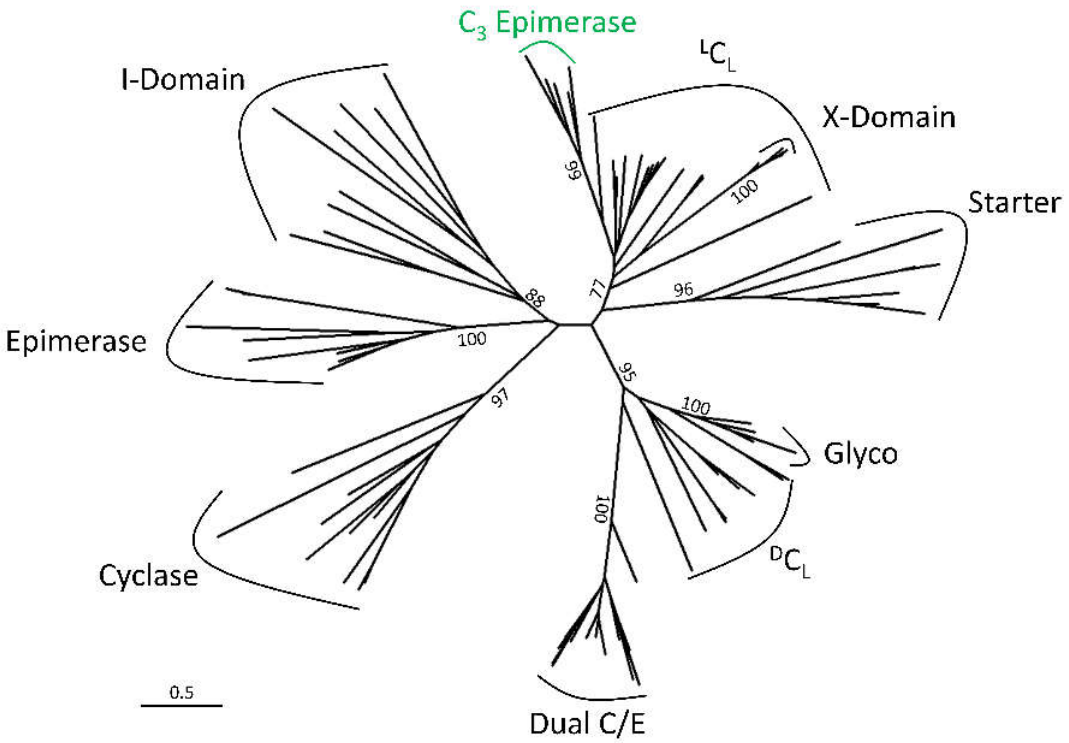

Figure S12. Phylogenetic tree of C domains from different datasets. The domains cluster depending on the specified function. $HynA_5C_2$ and homologues thereof form a new, distinct clade within the $^{L}C_L$ domains and probably catalyse C_3-epimerization (green). Bootstrap values indicate the distinctness of clades. The scale bar represents 50 substitutions per 100 amino acids.

SUPPORTING INFORMATION

Table S4. Accession numbers and source organisms of protein sequences used for phylogenetic analysis of C domains (Figure S12). If possible, accession numbers from Rausch et al.[5] were updated to NCBI nonredundant RefSeq (WP_).

Accession	Organism	Domain family	Ref.
WP_010924520.1	*Mycobacterium tuberculosis*	Cyclase	[5]
WP_010935625.1	*Corynebacterium diphtheriae*	Cyclase	[5]
WP_010949506.1	*Mycobacterium avium*	Cyclase	[5]
WP_002211388.1	*Yersinia pestis* CO92	Cyclase	[5]
WP_126987576.1	*Nostoc sp.* PCC 7120 = FACHB-418	Cyclase	[5]
CUV45544.1	*Ralstonia solanacearum*	Cyclase	[5]
WP_011030913.1	*Streptomyces coelicolor* A3(2)	Cyclase	[5]
AAN80883.1	*Escherichia coli* CFT073	Cyclase	[5]
WP_011146562.1	*Photorhabdus laumondii subsp. laumondii*	Cyclase	[5]
WP_011168195.1	*Pseudomonas savastanoi pv. phaseolicola*	Cyclase	[5]
WP_010895613.1	*Pseudomonas aeruginosa*	$^{D}C_{L}$	[5]
WP_010949130.1	*Mycobacterium avium subsp. paratuberculosis*	$^{D}C_{L}$	[5]
WP_011198677.1	*Bacillus cereus* E33L	$^{D}C_{L}$	[5]
WP_010949191.1	*Mycobacterium avium subsp. paratuberculosis*	$^{D}C_{L}$	[5]
WP_010954996.1	*Pseudomonas putida*	$^{D}C_{L}$	[5]
WP_011062374.1	*Pseudomonas protegens*	$^{D}C_{L}$	[5]
WP_011103865.1	*Pseudomonas syringae pv. tomato*	$^{D}C_{L}$	[5]
AAP09419	*Bacillus cereus* ATCC 14579	$^{D}C_{L}$	[5]
AAZ34524.1	*Pseudomonas savastanoi pv. phaseolicola* 1448A	$^{D}C_{L}$	[5]
CAD17793.1	*Ralstonia solanacearum* GMI1000	Dual C/E	[5]
WP_011060446.1	*Pseudomonas protegens*	Dual C/E	[5]
AND87649.1	*Bradyrhizobium diazoefficiens* USDA 110	Dual C/E	[5]
WP_011093070.1	*Pectobacterium atrosepticum* SCRI1043	Dual C/E	[5]
WP_011105127.1	*Pseudomonas syringae pv. tomato*	Dual C/E	[5]
WP_011136349.1	*Chromobacterium violaceum*	Dual C/E	[5]
WP_011146892.1	*Photorhabdus laumondii subsp. laumondii*	Dual C/E	[5]
WP_011204623.1	*Burkholderia mallei*	Dual C/E	[5]
WP_011205654.1	*Burkholderia pseudomallei* K96243	Dual C/E	[5]
WP_011104220.1	*Pseudomonas syringae pv. tomato*	Dual C/E	[5]
$HynA_3C$	*Lysobacter sp.* K5869	Dual C/E	[5]
$HynA_4C$	*Lysobacter sp.* K5869	Dual C/E	[5]
$HynA_6C$	*Lysobacter sp.* K5869	Dual C/E	[5]
WP_003916032.1	*Mycobacterium tuberculosis*	Epimerase	[5]
WP_010895613.1	*Pseudomonas aeruginosa*	Epimerase	[5]
WP_003412267.1	*Mycobacterium tuberculosis*	Epimerase	[5]
WP_010949130.1	*Mycobacterium avium subsp. paratuberculosis*	Epimerase	[5]
WP_010950704.1	*Mycobacterium tuberculosis variant bovis*	Epimerase	[5]
WP_010954975.1	*Pseudomonas putida*	Epimerase	[5]
NP_534179.1	*Agrobacterium tumefaciens* C58	Epimerase	[5]
WP_011062374.1	*Pseudomonas protegens*	Epimerase	[5]
AAP09415.1	*Bacillus cereus* ATCC 14579	Epimerase	[5]
AAQ59905.1	*Chromobacterium violaceum* ATCC 12472	Epimerase	[5]
AAM80537.1	*Streptomyces toyocaensis*	Glyco $^{L}C_{L}$	[5]
Q93N88	*Streptomyces lavendulae*	Glyco $^{L}C_{L}$	[5]
Q93N87	*Streptomyces lavendulae*	Glyco $^{L}C_{L}$	[5]
Q8KLL4	*Streptomyces toyocaensis*	Glyco $^{L}C_{L}$	[5]
AJF34464.1	*Eleftheria terrae*	C_3-epimerase	[17]
AEH59100.1	*Lysobacter sp.* ATCC 53042	C_3-epimerase	[22]
PRX87872.1	*Pseudomonas sp.* NFACC11-2	C_3-epimerase	[23]
CCJ67648.1	*Janthinobacterium agaricidamnosum*	C_3-epimerase	[24]
$HynA_5C_2$	*Lysobacter sp.* K5869	C_3-epimerase	This work
CAQ71827.1	*Cupriavidus taiwanensis* LMG 19424	I domain	[6]
CAJ96471.1	*Cupriavidus necator* H16	I domain	[6]
WP_063365585.1	*Pseudoalteromonas luteoviolacae*	I domain	[6]
WP_063365570.1	*Pseudoalteromonas luteoviolacae*	I domain	[6]
WP_082236112.1	*Cupriavidus necator*	I domain	[6]
WP_052269209.1	*Alcanivorax pacificus*	I domain	[6]
WP_029293154.1	*Pseudomonas sp.* 06C 126	I domain	[6]
WP_053122086.1	*Pseudomonas thivervalensis*	I domain	[6]
WP_053122092.1	*Pseudomonas thivervalensis*	I domain	[6]
AJW67534.1	*Pseudomonas taiwanensis*	I domain	[6]
WP_011534377.1	*Pseudomonas entomophila*	I domain	[6]
WP_003400794.1	*Mycobacterium tuberculosis*	$^{L}C_{L}$	[5]
WP_010895611.1	*Pseudomonas aeruginosa*	$^{L}C_{L}$	[5]
WP_000605281.1	*Staphylococcus aureus subsp. aureus*	$^{L}C_{L}$	[5]
WP_010949130.1	*Mycobacterium avium subsp. paratuberculosis*	$^{L}C_{L}$	[5]
WP_010954974.1	*Pseudomonas putida*	$^{L}C_{L}$	[5]
WP_000605273.1	*Staphylococcus aureus subsp. aureus*	$^{L}C_{L}$	[5]
BAC70870.1	*Streptomyces avermitilis* MA-4680 = NBRC 14893	$^{L}C_{L}$	[5]
WP_010996798.1	*Nostoc sp.* PCC 7120 = FACHB-418	$^{L}C_{L}$	[5]
CAD17793.1	*Ralstonia solanacearum* GMI1000	$^{L}C_{L}$	[5]
WP_010973240.1	*Agrobacterium fabrum*	$^{L}C_{L}$	[5]
$HynA_2C$	*Lysobacter sp.* K5869	$^{L}C_{L}$	[5]
$HynA_5C_1$	*Lysobacter sp.* K5869	$^{L}C_{L}$	[5]
$HynB_7C$	*Lysobacter sp.* K5869	$^{L}C_{L}$	[5]
$HynB_8C$	*Lysobacter sp.* K5869	$^{L}C_{L}$	[5]

Table S4 (continuation). Accession numbers and source organisms of protein sequences used for phylogenetic analysis of C domains. If possible, accession numbers from Rausch et al.[5] were updated to NCBI nonredundant RefSeq (WP_).

Accession	Organism	Domain family	Ref.
WP_000077805.1	*Escherichia coli* K12	Starter	[5]
AAD56240.1	*Bacillus subtilis*	Starter	[5]
WP_003113143.1	*Pseudomonas aeruginosa*	Starter	[5]
WP_010949130.1	*Mycobacterium avium subsp. paratuberculosis*	Starter	[5]
BAC68313.1	*Streptomyces avermitilis* MA-4680 = NBRC 14893	Starter	[5]
WP_000194139.1	*Salmonella typhimurium*	Starter	[5]
WP_001133934.1	*Bacillus cereus*	Starter	[5]
AEI58867.1	*Amycolatopsis orientalis* HCCB10007	X domain	[25]
CAC48362.1	*Amycolatopsis balhimycina* DSM 5908	X domain	[25]
CAG15012.1	*Actinoplanes teichomyceticus*	X domain	[25]
CAD91211.1	*Nonomuraea gerenanesis*	X domain	[25]

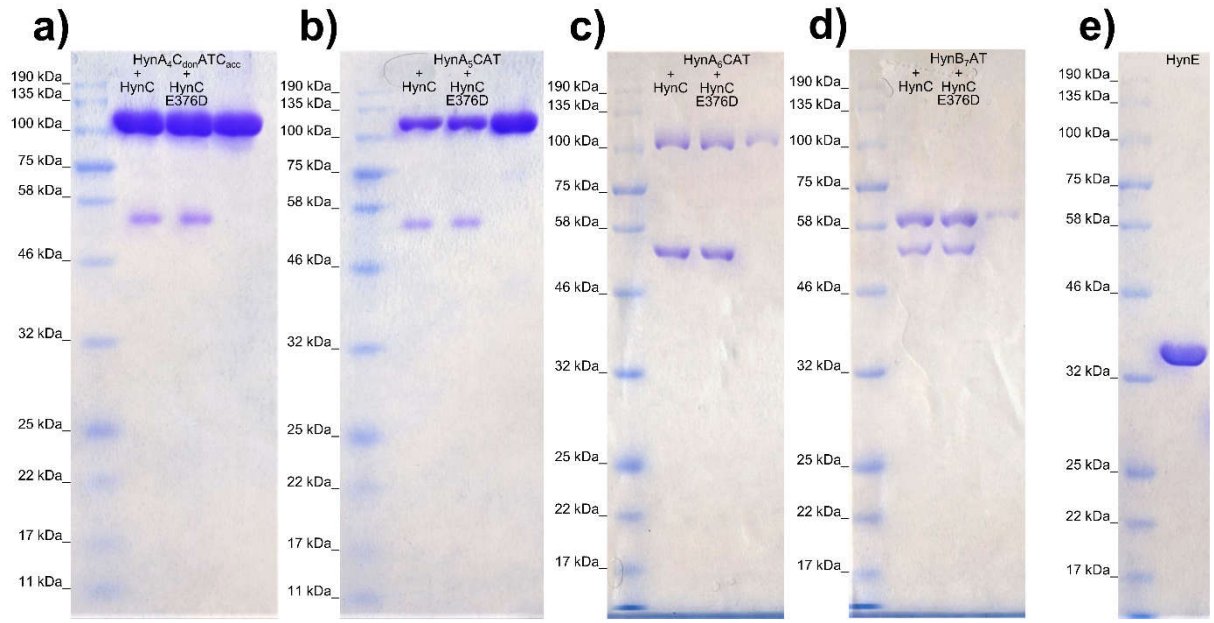

Figure S13. SDS-PAGEs of heterologously expressed enzymes. a) $HynA_4C_{acc}ATC_{don}$ (117.7 kDa) co-expressed with HynC (63.2 kDa), HynC E376D (63.7 kDa) and alone. b) $HynA_5CAT$ (122. kDa) co-expressed with HynC, HynC E376D and alone. c) $HynA_6CAT$ (117.5 kDa) co-expressed with HynC, HynC E376D and alone. d) $HynB_7AT$ (66.9 kDa) co-expressed with HynC, HynC E376D and alone. e) HynE (38.8 kDa).

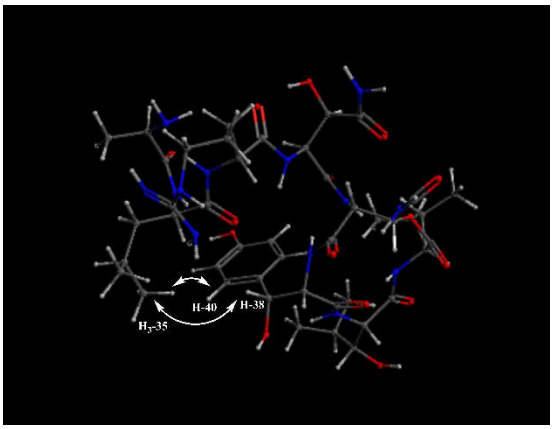

Figure S14. Conformation of **1**; white arrows indicate key ROESY correlations, supporting the (*2S*,3*R*) configuration of 3-Hydroxytyrosine, instead of (*2S*,3S).

SUPPORTING INFORMATION

Bioactivity of 1

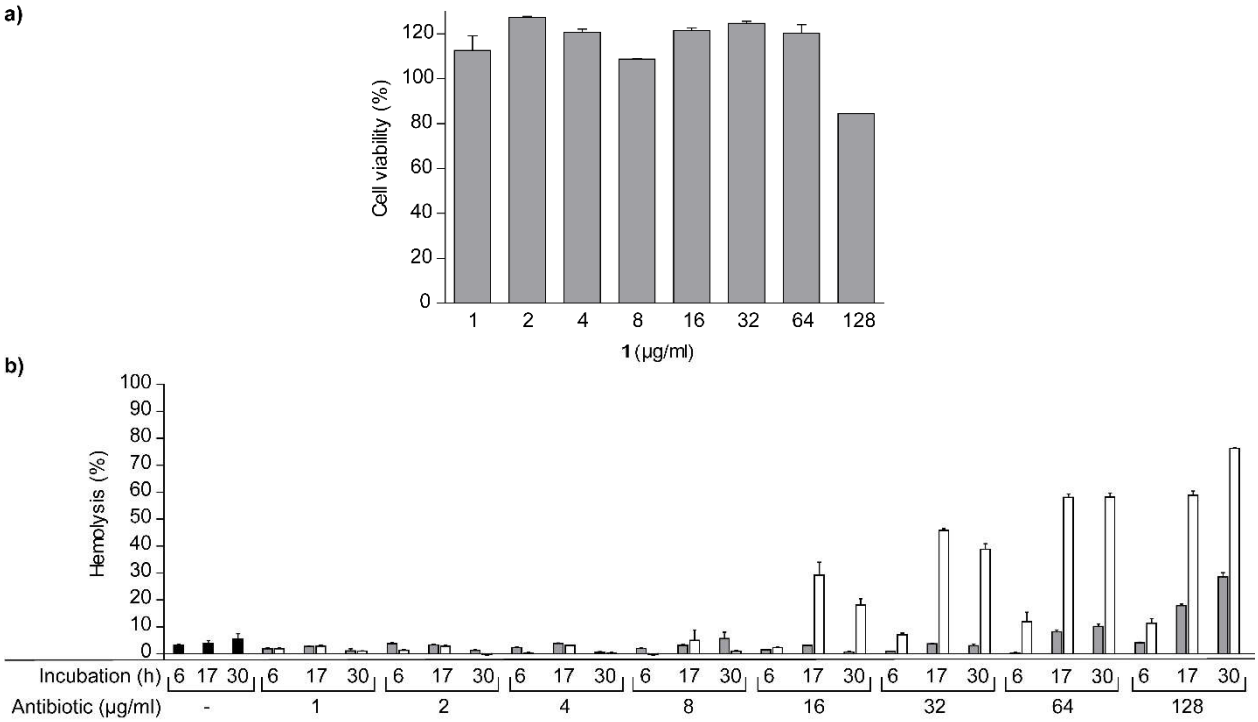

Figure S15. Cytotoxicity and hemolysis. a) Cytotoxicity of **1** against HEp-2 cells. HEp-2 cells were incubated with serially diluted concentrations of **1** for 30 h. Metabolically active cells reduced resazurin to resorufin and absorbance was measured. **1** did not show cytotoxic effects up to 64 µg/mL. b) Human RBC hemolysis following treatment with **1** (*grey bars*) and teixobactin (*white bars*) expressed relative to Triton X-100-induced RBC lysis (set 100 %). Cells left untreated are shown with *black bars*. RBCs were challenged with serially diluted concentrations of antibiotics for 6, 17, and 30 h, respectively. **1** exhibited low hemolytic activity towards RBCs and was inferior to teixobactin within the tested range up to 128 µg/ml. Error bars indicate ±standard deviation (*n* = 3).

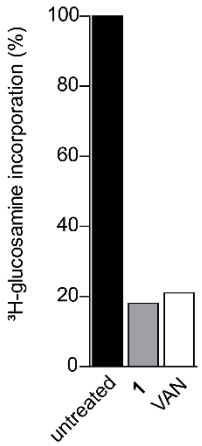

Figure S16. 1 (1× MIC, *grey bar*) inhibits incorporation of ^{3}H-glucosamine into the cell wall of *S. aureus* cells. Vancomycin (10× MIC) was used as control (*white bar*). The untreated control is shown as *black bar*.

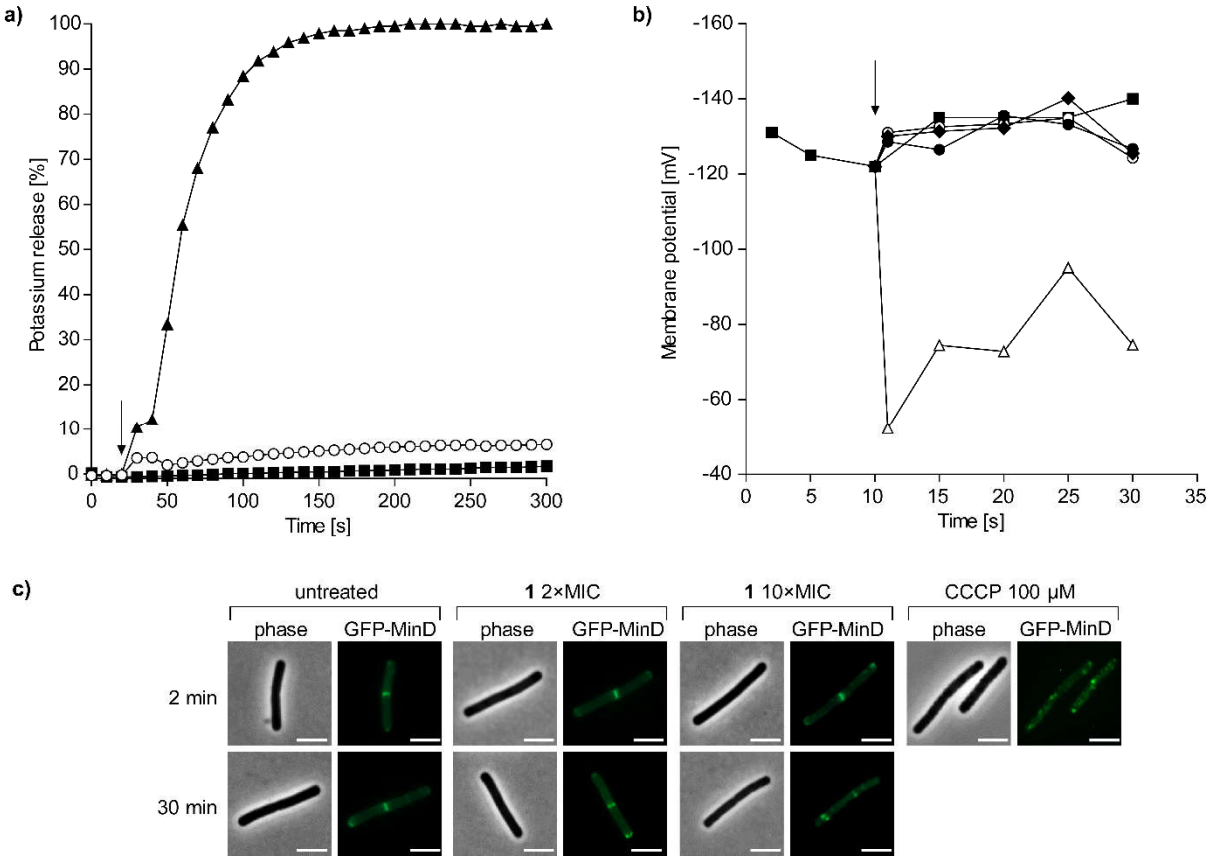

Figure S17. Impact of **1** on membrane potential a) **1** (1× MIC, *open circles*) is unable to form pores in the cytoplasmic membrane of *S. simulans* 22. Potassium efflux from living cells was monitored with a potassium-sensitive electrode. Ion leakage is expressed relative to the total amount of potassium released after addition of 1 µM pore-forming lantibiotic nisin (100 %, *triangles*). b) **1** does not affect membrane integrity or membrane potential. **1** shows no influence on the membrane potential of *S. simulans* 22 compared to the ionophore carbonyl cyanide *m*-chlorophenylhydrazone (CCCP, *open triangles*). The membrane potential was calculated from the distribution of the lipophilic cation TPP^+ inside and outside the cells. **1** was added at 1× MIC (*open circles*), 2× MIC (*circles*), and 5× MIC (*diamonds*). Untreated cells (*squares*). Arrows indicate the time of antibiotic or CCCP addition, respectively. c) Fluorescence microscopy revealed that **1** does not induce delocalization of membrane-potential driven GFP-MinD in early exponential phase cultures of *B. subtilis*. The ionophore CCCP was used as positive control. Scale bar = 5 µm.

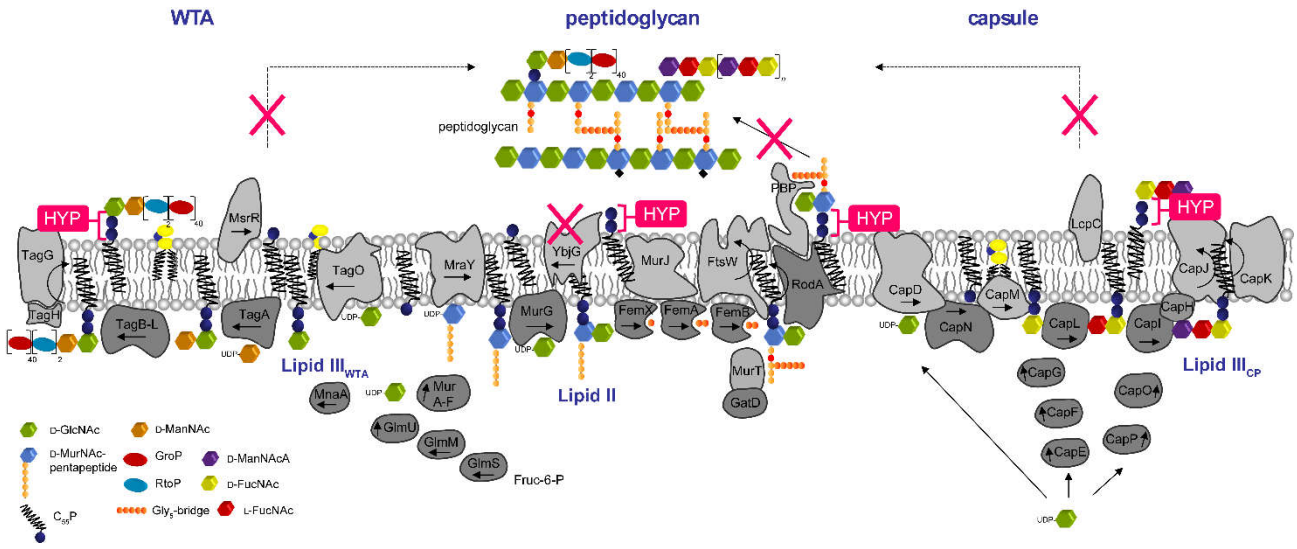

Figure S18. Cell wall biosynthesis network of *S. aureus*. Building up a vital cell wall requires the precise spatio-temporal coordination of multienzyme machineries of peptidoglycan, wall teichoic acid (WTA) and capsule biosynthesis, that consume intimately shared precursors, such as $C_{55}P$. Hypeptin (pink) interferes with these processes by binding to $C_{55}PP$-containing precursors. HYP, hypeptin; WTA, wall teichoic acid; CP, capsular polysaccharide; GlcNAc, *N*-acetyl-glucosamine; MurNAc, *N*-acetyl-muramic acid; ManNAc, *N*-acetyl-mannosamine; ManNAcA, *N*-acetyl-mannosaminuronic acid; FucNAc, *N*-acetyl-fucosamine; GroP, glycerol phosphate; RtoP, ribitol phosphate; Gly_5, pentaglycine; UDP, uridine-5'-diphosphate; Fruc-6-P, fructose-6-phosphate.

Table S5. Antagonization of the antimicrobial activity of **1** and teixobactin by cell wall precursors. *S. aureus* was incubated with **1**, TEIX and VAN at 8× MIC in nutrient broth in microtiter plates, and growth was measured after a 24 h incubation at 37 °C. Putative HPLC-purified antagonists (undecaprenyl-phosphate [$C_{55}P$], geranylgeranyl-phosphate [$C_{20}P$], geranylgeranyl-pyrophosphate [$C_{20}PP$], undecaprenyl-pyrophosphate [$C_{55}PP$], lipid I, lipid II, and lipid III_{WTA}) and 1,2-dioleoyl-sn-glycero-3-phospho-glycerol (DOPG) were added in a fivefold molar excess with respect to the antibiotic. Experiments were performed with biological replicates. + antagonization; - no antagonization.

	Molar ratio lipid : antibiotic		
Lipid	**1**	**TEIX**	**VAN**
$C_{20}P$	–	–	–
$C_{55}P$	–	–	–
$C_{20}PP$	+ (4:1)	+ (4:1)	–
$C_{55}PP$	+ (4:1)	+ (4:1)	–
lipid I	+ (1:1)	+ (1:1)	+ (1:1)
lipid II	+ (1:1)	+ (1:1)	+ (1:1)
lipid III_{WTA}	+ (1:1)	+ (1:1)	–
DOPG	–	–	–

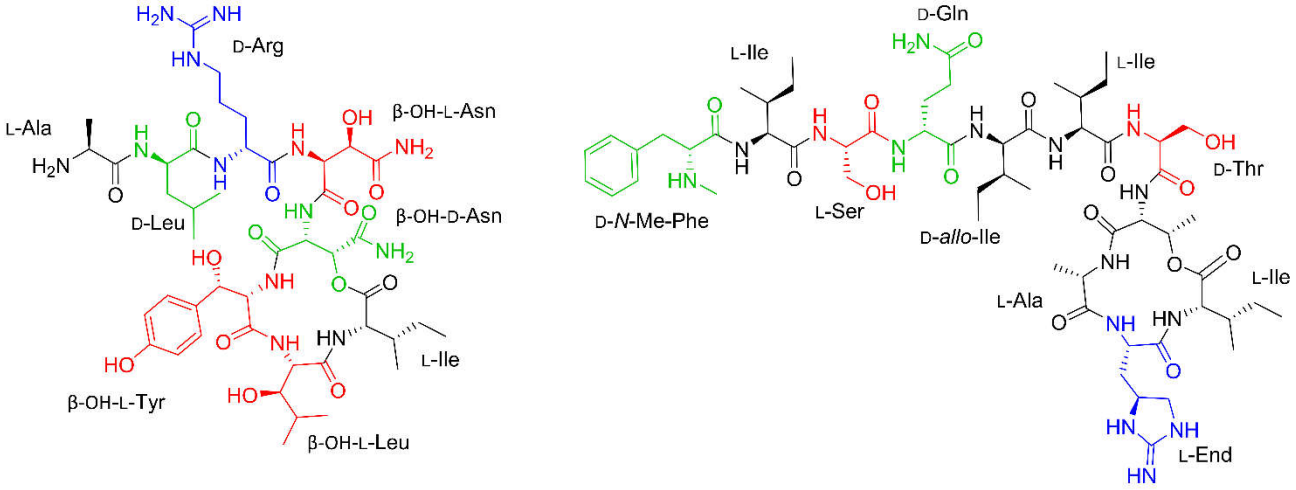

Figure S19. Structural comparison of **1** (left) with teixobactin (right). Both antibiotics are cyclodepsipeptides, consisting of guanidine amino acids (blue), β-hydroxy amino acids (red), D-configurated amino acids (green), and branched aliphatic amino acids. Adapted from Nussbaum and Süssmuth.[26]

SUPPORTING INFORMATION

References

[1] E. Gavrish, C. S. Sit, S. Cao, O. Kandror, A. Spoering, A. Peoples, L. Ling, A. Fetterman, D. Hughes, A. Bissell et al., *Chem Biol.* **2014**, *21*, 509.
[2] H. Harms, A. Klöckner, J. Schrör, M. Josten, S. Kehraus, M. Crüsemann, W. Hanke, T. Schneider, T. F. Schäberle, G. M. König, *Planta Med.* **2018**, *84*, 1363.
[3] D. G. Gibson, L. Young, R.-Y. Chuang, J. C. Venter, C. A. Hutchison, H. O. Smith, *Nat Methods.* **2009**, *6*, 343.
[4] V. V. Phelan, Y. Du, J. A. McLean, B. O. Bachmann, *Chem Biol.* **2009**, *16*, 473.
[5] C. Rausch, I. Hoof, T. Weber, W. Wohlleben, D. H. Huson, *BMC Evol. Biol.* **2007**, *7*, 78.
[6] Z. L. Reitz, C. D. Hardy, J. Suk, J. Bouvet, A. Butler, *Proc Natl Acad Sci U S A.* **2019**, *116*, 19805.
[7] S. Kumar, G. Stecher, M. Li, C. Knyaz, K. Tamura, *Mol Biol Evol.* **2018**, *35*, 1547.
[8] S. Tan, K. C. Ludwig, A. Müller, T. Schneider, J. R. Nodwell, *ACS Chem Biol* **2019**, *14*, 966.
[9] C. Freiberg, N. A. Brunner, G. Schiffer, T. Lampe, J. Pohlmann, M. Brands, M. Raabe, D. Häbich, K. Ziegelbauer, *J Biol Chem.* **2004**, *279*, 26066.
[10] T. Schneider, T. Kruse, R. Wimmer, I. Wiedemann, V. Sass, U. Pag, A. Jansen, A. K. Nielsen, P. H. Mygind, D. S. Raventós et al., *Science* **2010**, *328*, 1168.
[11] C. A. Schneider, W. S. Rasband, K. W. Eliceiri, *Nat Methods* **2012**, *9*, 671.
[12] a) A. Müller, M. Wenzel, H. Strahl, F. Grein, T. N. V. Saaki, B. Kohl, T. Siersma, J. E. Bandow, H.-G. Sahl, T. Schneider et al., *Proc Natl Acad Sci U S A.* **2016**, *113*, E7077-E7086; b) H. Strahl, L. W. Hamoen, *Proc Natl Acad Sci U S A.* **2010**, *107*, 12281.
[13] E. Ruhr, H. G. Sahl, *Antimicrob Agents Chemother.* **1985**, *27*, 841.
[14] D. S. Orlov, T. Nguyen, R. I. Lehrer, *J Microbiol Methods.* **2002**, *49*, 325.
[15] U. Kohlrausch, J. V. Höltje, *J Bacteriol.* **1991**, *173*, 3425.
[16] T. Schneider, K. Gries, M. Josten, I. Wiedemann, S. Pelzer, H. Labischinski, H.-G. Sahl, *Antimicrob. Agents Chemother.* **2009**, *53*, 1610.
[17] a) L. L. Ling, T. Schneider, A. J. Peoples, A. L. Spoering, I. Engels, B. P. Conlon, A. Mueller, T. F. Schäberle, D. E. Hughes, S. Epstein et al., *Nature.* **2015**, *517*, 455; b) A. Müller, H. Ulm, K. Reder-Christ, H.-G. Sahl, T. Schneider, *Microb Drug Resist.* **2012**, *18*, 261.
[18] G. Rouser, S. Fkeischer, A. Yamamoto, *Lipids.* **1970**, *5*, 494.
[19] a) J. N. Umbreit, J. L. Strominger, *J Bacteriol.* **1972**, *112*, 1306; b) H. Brötz, G. Bierbaum, K. Leopold, P. E. Reynolds, H. G. Sahl, *Antimicrob Agents Chemother.* **1998**, *42*, 154.
[20] P. D. Rick, G. L. Hubbard, M. Kitaoka, H. Nagaki, T. Kinoshita, S. Dowd, V. Simplaceanu, C. Ho, *Glycobiology.* **1998**, *8*, 557.
[21] T. Schneider, M. M. Senn, B. Berger-Bächi, A. Tossi, H.-G. Sahl, I. Wiedemann, *Mol Microbiol.* **2004**, *53*, 675.
[22] J. Hou, L. Robbel, M. A. Marahiel, *Chem Biol.* **2011**, *18*, 655.
[23] B. K. Scholz-Schroeder, J. D. Soule, D. C. Gross, *Mol Plant Microbe Interact.* **2003**, *16*, 271.
[24] K. Graupner, K. Scherlach, T. Bretschneider, G. Lackner, M. Roth, H. Gross, C. Hertweck, *Angew Chemie Int Ed. Engl.* **2012**, *51*, 13173.
[25] K. Haslinger, M. Peschke, C. Brieke, E. Maximowitsch, M. J. Cryle, *Nature.* **2015**, *521*, 105.
[26] F. von Nussbaum, R. D. Süssmuth, *Angew. Chem. Int Ed. Engl.* **2015**, *54*, 6684-6686.

Author Contributions

L.L.L., A.L.S, A.J.P, A.N. and K.L. isolated *Lysobacter sp.* K5869 and **1**;
D.A.W. performed all BCG cloning, in vitro experiments, and bioinformatic analyses under supervision of M.C.;
D.A.W. and P.B. assembled and analyzed the genome of *Lysobacter sp.* K5869.;
M.A., C.E.M. and M.J. optimized growth conditions and purified **1** under supervision of T.S., K.L., A.J.P. and L.L.L.;
P.B. characterized **1** under supervision of G.M.K.;
S.Ke. and D.A.W. elucidated the structure of **1**;
K.C.L., M.A., C.E.M. and A.M. performed mode of action analysis under supervision of T.S.;
S.Kr. performed cytotoxicity assays under supervision of B.H.;
The manuscript was written by T.S. and M.C. with contributions by all authors.